Supporting information for:

Spray deposition of $AgBiS_2$ and Cu_3BiS_3 thin films for photovoltaic applications

Narendra Pai[a], Jianfeng Lu[a], Dimuthu C. Senevirathna[a], Anthony S. R. Chesman[b], Thomas Gengenbach[b], Manjunath Chatti[ac], Udo Bach[b,d,e], Philip C. Andrews[a], Leone Spiccia[a,c], Yi-Bing Cheng[f,g], and Alexandr N. Simonov[a,c]

[a] School of Chemistry, Monash University, Melbourne, Victoria, 3800, Australia

[b] Commonwealth Scientific and Industrial Research Organisation Manufacturing, Clayton, Victoria 3168, Australia

[c] ARC Centre of Excellence for Electromaterials Science, Monash University, Melbourne, Victoria, 3800, Australia

[d] ARC Centre of Excellence in Exciton Science and Department of Chemical Engineering, Monash University, Melbourne, Victoria, 3800, Australia

[e] The Melbourne Centre for Nanofabrication, Clayton, Victoria 3168, Australia

[f] ARC Centre of Excellence in Exciton Science and Department of Materials Science and Engineering, Monash University, Melbourne, Victoria, 3800, Australia.

[g] State Key Laboratory of Advanced Technology for Materials Synthesis and Processing, Wuhan University of Technology, Wuhan 430070, China

TABLE OF CONTENTS

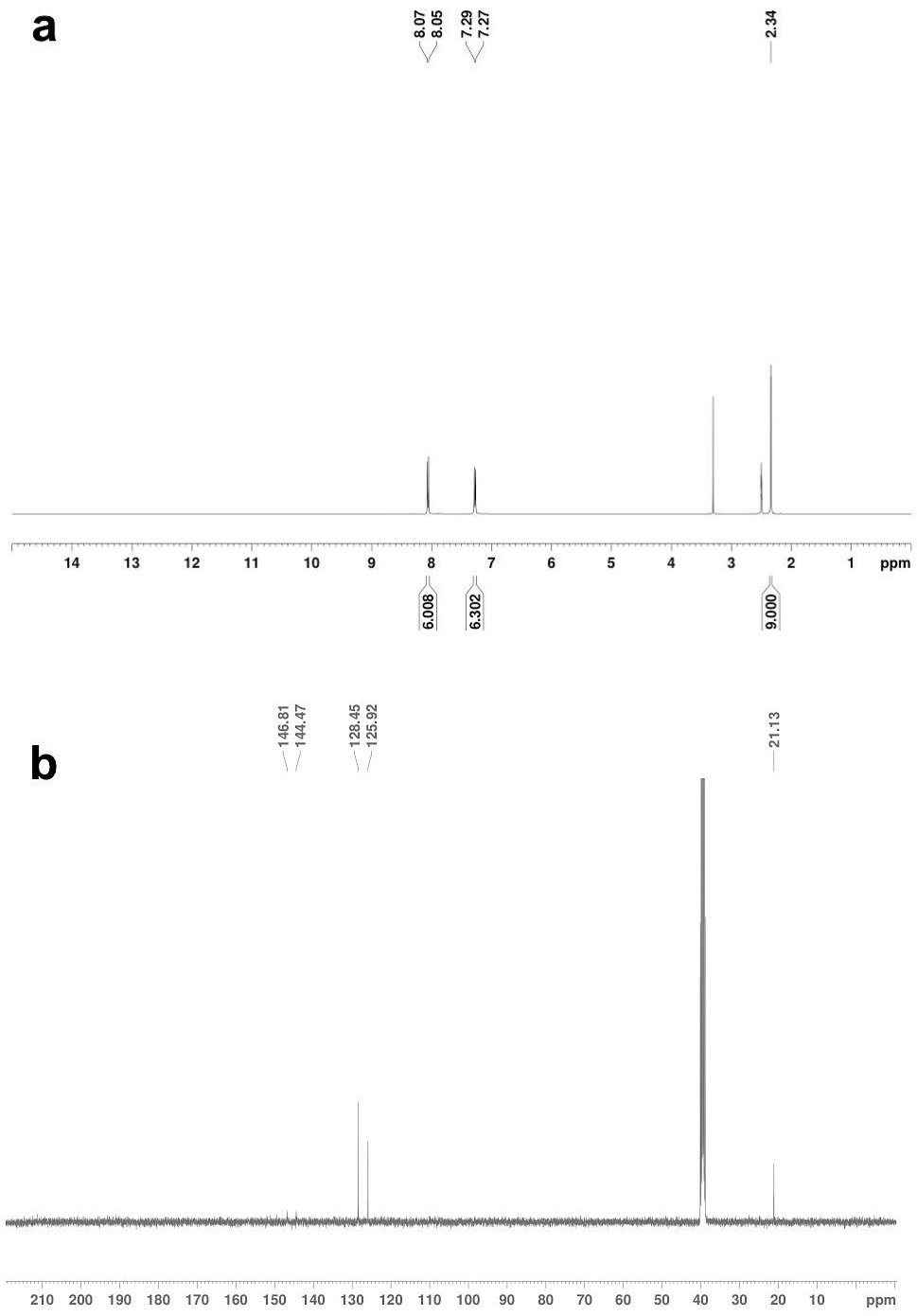

Figure S1. (a) ^{1}H- and (b) ^{13}C-NMR spectra of bismuth 4-methyl benzoditholate $[Bi(4\text{-}MBDT)_3]$ in d_6-DMSO. HR-MS $(ESI)^+$ m/z 543 $[Bi(S_2C(C_6H_4)\text{-}4\text{-}CH_3)_2]^+$. Elemental analysis for $C_{24}H_{21}BiS_6$: calculated: C 40.56, H 2.98; found: C 40.43, H 2.81.

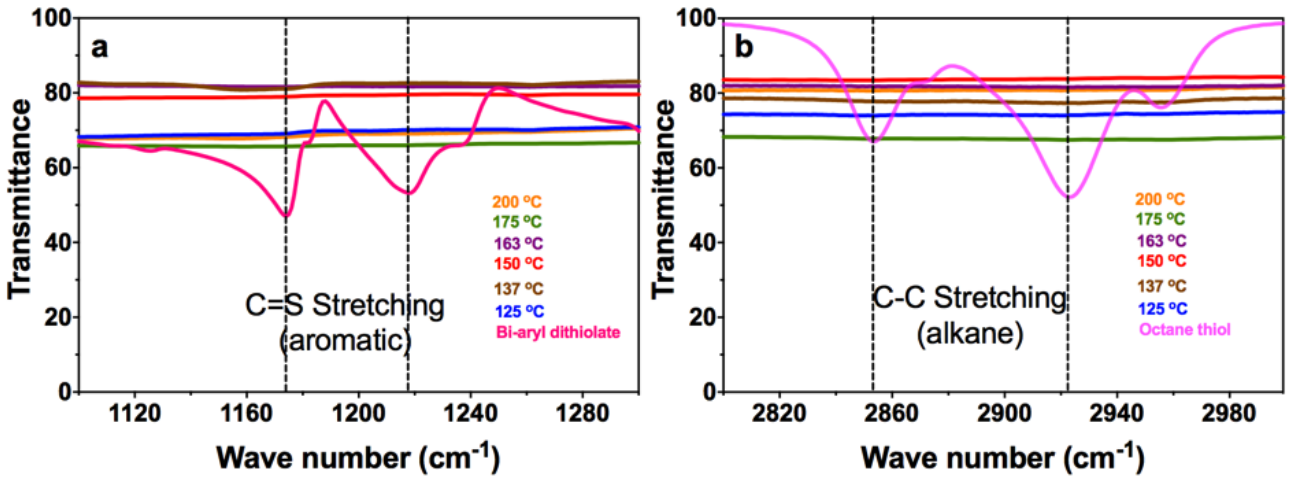

Figure S2. Selected ranges of the FTIR spectra of $AgBiS_2$ films spray-deposited onto glass at different temperatures: (a) 1100-1300 cm^{-1} range relevant to the aromatic C=S stretching bands (1175 and 1220 cm^{-1}, dashed lines), and (b) 2800-3000 cm^{-1} range relevant to the C–C stretching bands (2845 and 2915 cm^{-1}, dashed lines). *Pink* and *magenta* curves show spectra for (a) bismuth(III) tris(methyl-benzodithiolate) and (b) 1-octanethiol.

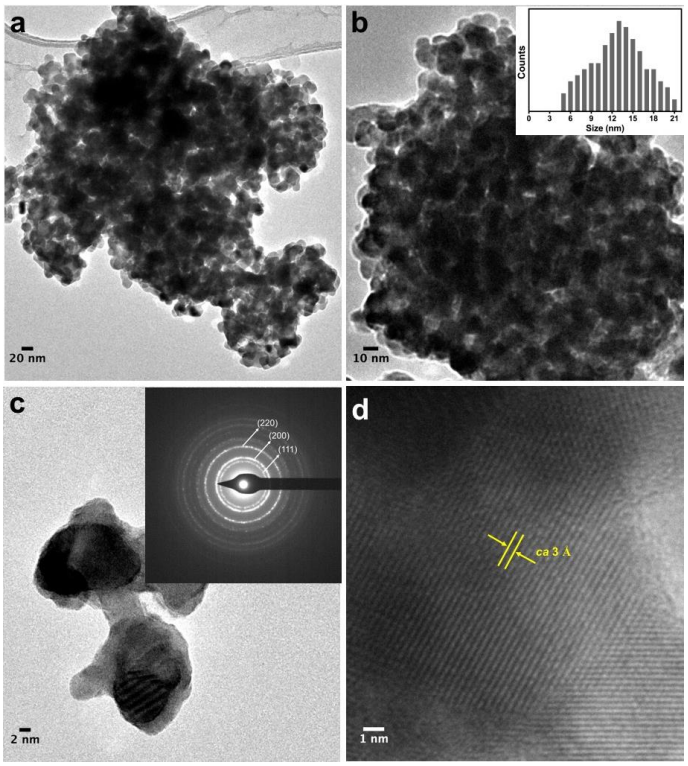

Figure S3. (a-c) TEM and (d) HRTEM images of $AgBiS_2$ spray-deposited onto glass at 150 °C (the material was scratched from the support to be analysed by TEM). Inset in panel **b** shows a particle size distribution histogram based on 100 particles. Inset in panel **c** shows an indexed SAED pattern.

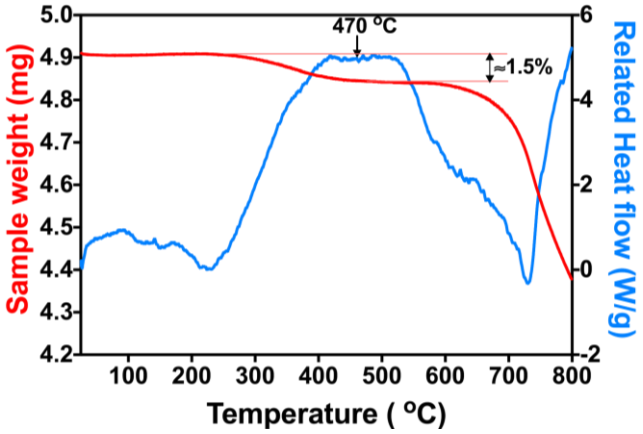

Figure S4. TGA-DSC plot obtained under high-purity Ar atmosphere for the $AgBiS_2$ sample spray-deposited onto ZnO|ITO at 150 °C (the material was scratched from the support surface for the analysis). Sample weight loss and heat flow data are shown as *red* and *blue* curves, respectively.

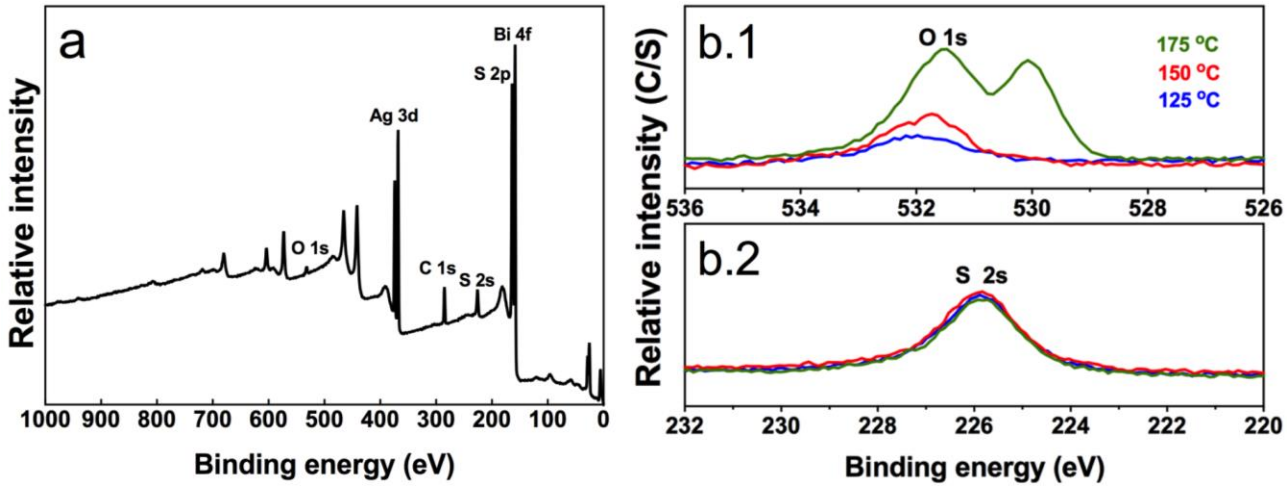

Figure S5. (a) Survey XP spectrum, (b.1) high resolution O 1s and (b.2) S 2s spectra of $AgBiS_2$ spray-deposited onto ITO at (a) 150 °C or (b) 125 (*blue*), 150 (*red*) and 175 °C (*green*).

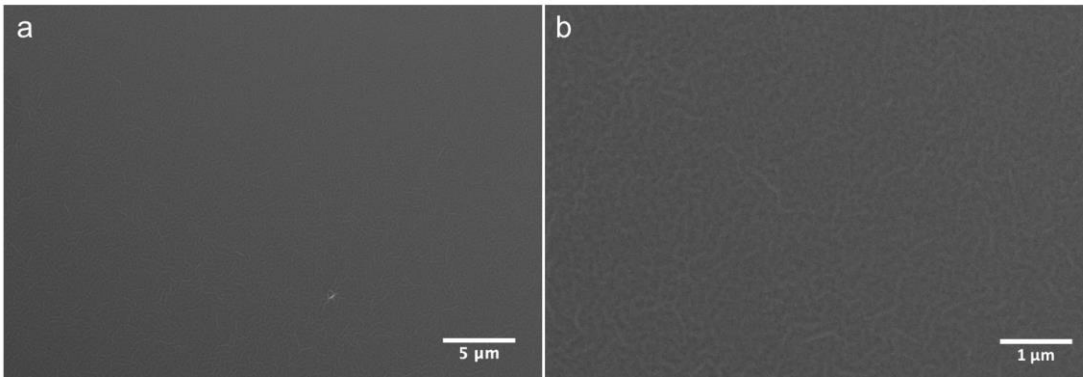

Figure S6. (a) Lower and (b) higher magnification SEM top-view images of a ZnO film on an ITO support.

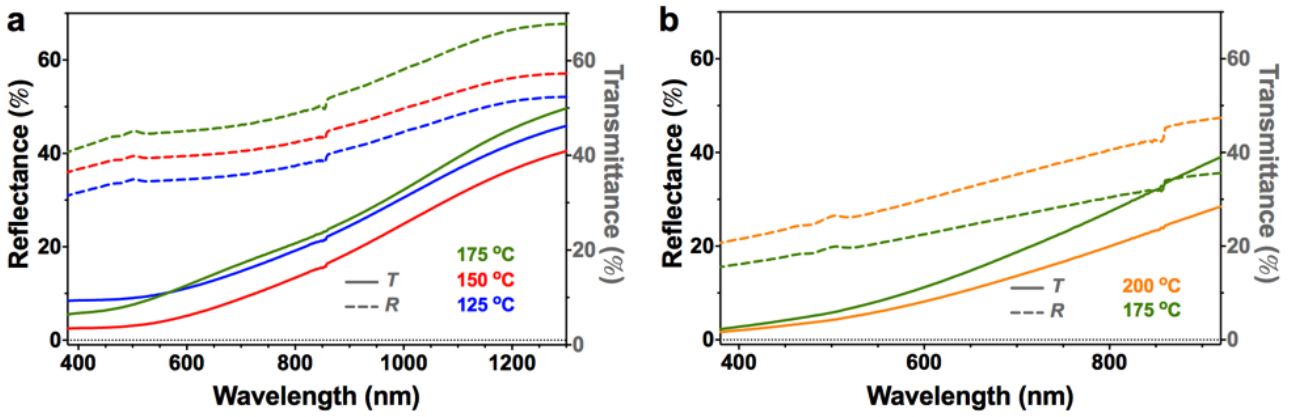

Figure S7. Reflectance (*R*, dashed lines) and transmittance (*T*, solid lines) of (a) $AgBiS_2$ and (b) Cu_3BiS_3 films spray-deposited on glass at 125 (*blue*), 150 (*red*), 175 (*green*) and 200 °C (*orange*).

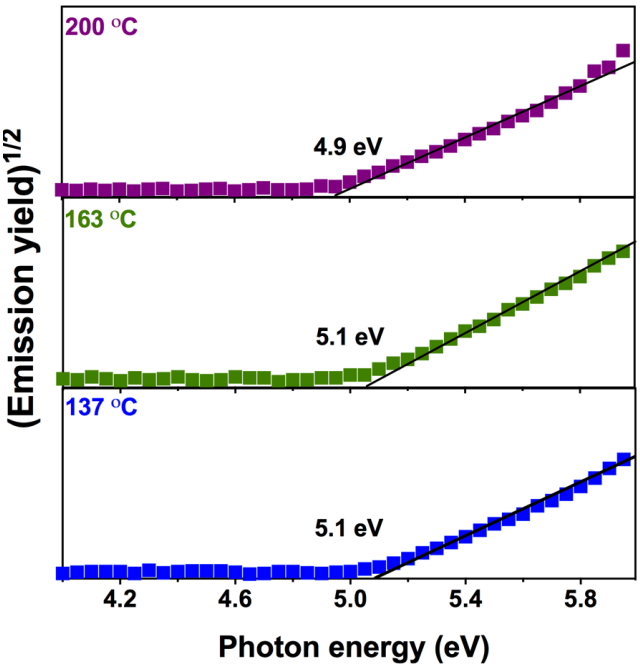

Figure S8. PESA data obtained for the $AgBiS_2$ films deposited by spray pyrolysis onto glass substrate at 125 (*blue*), 150 (*red*) and 175 °C (*green*). Black lines show linear fits to the data used to derive E_{VB}.

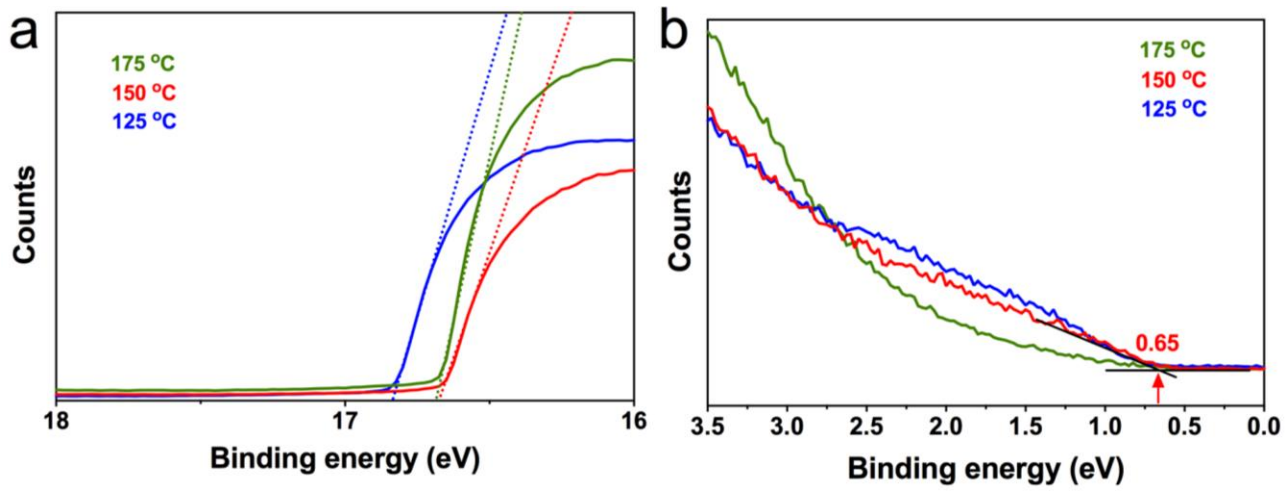

Figure S9. (a) Higher and (b) lower binding energy regions of the ultra-violet photoelectron spectra obtained for $AgBiS_2$ films spray-deposited onto ITO at 125 (*blue*), 150 (*red*) and 175 °C (*green*). *Dotted* lines in panel **a** and *solid black* lines in panel **b** show linear fits used to derive secondary electron cut-off and HOMO cut-off, respectively.

Table S1. Parameters derived from the analysis of the UPS data obtained for $AgBiS_2$ films spray-deposited onto ITO at different temperatures.

Deposition temperature (°C)	Secondary electron cut-off (eV) [a]	Work function (eV) [b]	HOMO cut-off (eV) [a]	Ionisation potential (eV) [c]
125	16.82	-4.40	-0.75	-5.15
150	16.66	-4.56	-0.65	-5.21
175	16.66	-4.56	-0.60	-5.16

[a] Derived from experimental data as exemplified in Figure S9. [b] Calculated as difference between an incident photon energy (21.22 eV) and secondary electron cut-off. [c] Calculated as a difference between work function and HOMO cut-off; ionisation potential serves as a reasonably accurate estimate of the valence band energy level.[S1]

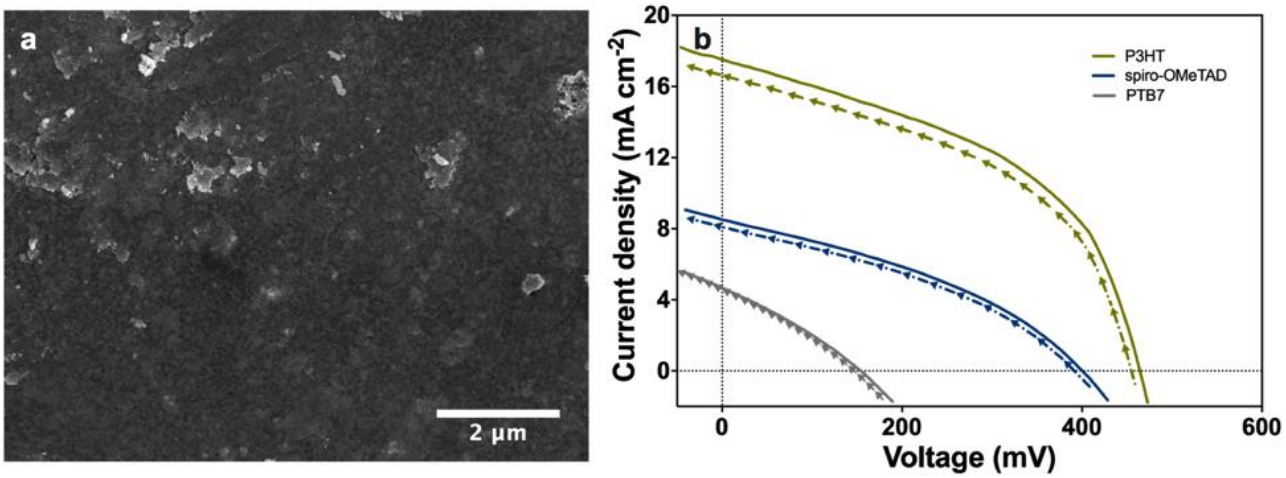

Figure S10. Characterisation of a $AgBiS_2$ thin layer and $AgBiS_2$-based solar cells fabricated following the procedures reported by Bernechea *et al.*[S2]: (a) SEM top-view image of the $AgBiS_2$ film on ZnO|ITO; (b) photocurrent-voltage curves (scan rate 100 mV s^{-1}) measured under 1 sun AM1.5G irradiation for the Au|MoO_3+HTM|$AgBiS_2$|ZnO|ITO devices (aperture 0.16 cm^2) with spiro-OMeTAD (*tan*), P3HT (*blue*) or PTB7 (*grey*) as a HTM. Dashed lines with arrows and solid lines show reverse and forward bias scanning, respectively. Dotted lines are guides to the eye showing zero *J* and *V*.

Table S2. Photovoltaic parameters[a] for planar Ag|MoO_3+spiro-OMeTAD|$AgBiS_2$|ZnO|ITO solar cells with the light absorber layer prepared as reported in Ref.[S2] under 1 sun AM1.5G irradiation (aperture 0.16 cm^2).

HTM	Ref.	V_{oc} (mV)	J_{SC} (mA cm^{-2})	FF (%)	PCE (%)
spiro- OMeTAD	Bernechea *et al.*[S2]	420	6.60	42	1.16
	This work[b]	394 ± 6	8.0 ± 0.1	37.0 ± 0.2	1.2 ± 0.1
P3HT	Bernechea *et al.*[S2]	460	15.1	57	3.99
	This work[b]	454 ± 6	16.5 ± 0.2	45.0 ± 0.2	3.5 ± 0.1
PTB7	Bernechea *et al.*[S2]	460 ± 10	17.5 ± 1.4	60±3	4.8 ± 0.4
	This work[b]	145 ± 4	4.5 ± 0.2	30.0 ± 0.4	0.20 ± 0.05

[a] Derived from the *J-V* curves (sweep rate 100 mV s^{-1}) for 10 devices of each type with an aperture of 0.16 cm^2; V_{oc} - open circuit voltage, J_{sc} – short circuit current density, FF – fill factor, PCE – power conversion efficiency. [b] Devices reproduced in our laboratory.

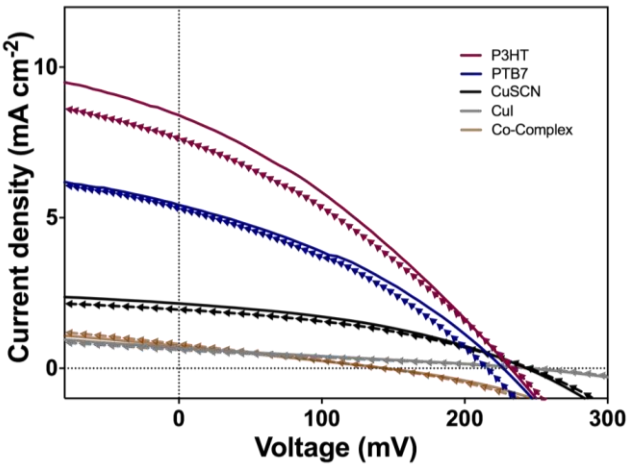

Figure S11. (a) Photocurrent-voltage curves (scan rate 100 mV s^{-1}) measured under 1 sun AM1.5G irradiation for the Ag|HTM|$AgBiS_2$|ZnO|ITO devices based on the $AgBiS_2$ films spray-deposited at 150 °C and with P3HT+MoO_3 (*maroon*), PTB7+MoO_3 (*indigo*), CuSCN (*black*), CuI (*grey*) and [Co(bpyPY$_4$)](OTf)$_{2.66}$ (*brown*) as HTM. Dashed lines with arrows and solid lines show reverse and forward bias scanning, respectively. Dotted lines are guides to the eye showing zero *J* and *V*.

Table S3. Photovoltaic parameters[a] of the planar Ag|HTM|$AgBiS_2$|ZnO|ITO solar cells with different hole transport layers under 1 sun AM1.5G irradiation (aperture 0.16 cm^2).

HTM	V_{oc} (mV)	J_{SC} (mA cm^{-2})	FF (%)	PCE (%)
P3HT + MoO_3	228 ± 5	8.3 ± 0.1	32 ± 1	0.6 ± 0.1
PTB7 + MoO_3	216 ± 4	5.3 ± 0.1	34 ± 1	0.4 ± 0.1
CuSCN	239 ± 4	2.2 ± 0.1	36 ± 0	0.2 ± 0.0
CuI	238 ± 8	0.8 ± 0.1	32 ± 0	0.07 ± 0.04
[Co(bpyPY4)](OTf)$_{2.66}$	143 ± 5	0.9 ± 0.3	28 ± 1	0.04 ± 0.02
Spiro-OMeTAD + MoO_3	241 ± 7	18.1 ± 0.6	35 ± 1	1.5 ± 0.1

[a] Derived from the *J-V* curves (sweep rate of 100 mV s^{-1}) for 10 devices of each type with an aperture of 0.16 cm^2; V_{oc} - open circuit voltage, J_{sc} – short circuit current density, FF – fill factor, PCE – power conversion efficiency.

Table S4. Photovoltaic parameters[a] of the planar Ag|(MoO_3+)spiro-OMeTAD|$AgBiS_2$|ZnO|ITO solar cells with the light absorber formed by spray pyrolysis at different temperatures under 1 sun irradiation.

T_{dep} (°C)	MoO_3[b]		V_{oc} (mV)	J_{sc} (mA cm^{-2})	FF (%)	PCE (%)
125	N	SC to OC[c]	194 ± 3	9.6 ± 0.2	32.6 ± 0.4	0.61 ± 0.03
		OC to SC[c]	191 ± 4	9.5 ± 0.3	32.1 ± 0.5	0.58 ± 0.04
		Best[d]	200	9.7	32.9	0.64
	Y	SC to OC	230 ± 3	10.8 ± 0.4	32.8 ± 0.5	0.78 ± 0.03
		OC to SC	227 ± 2	10.5 ± 0.3	31.9 ± 0.4	0.76 ± 0.03
		Best	231	10.6	33.0	0.81
137	N	SC to OC	197 ± 4	12.6 ± 0.4	32.8 ± 0.4	0.82 ± 0.03
		OC to SC	193 ± 4	12.5 ± 0.3	32.4 ± 0.5	0.78 ± 0.06
		Best	203	12.8	33.1	0.86
	Y	SC to OC	236 ± 4	14.7 ± 0.4	33.0 ± 0.3	1.14 ± 0.05
		OC to SC	234 ± 3	13.8 ± 0.5	33.2 ± 0.2	1.08 ± 0.07
		Best	237	15.1	33.2	1.19
150	N	FB to SC	201 ± 5	15.4 ± 0.3	33.7 ± 0.3	1.04 ± 0.05
		SC to FB	199 ± 3	14.6 ± 0.5	33.5 ± 0.4	0.98 ± 0.07
		Best	207	15.7	34.1	1.11
	Y	SC to OC	241 ± 7	18.1 ± 0.6	34.6 ± 0.5	1.50 ± 0.12
		OC to SC	239 ± 4	17.9 ± 0.5	34.4 ± 0.2	1.46 ± 0.07
		Best	251	18.9	35.8	1.69
		Best (1 cm^2)[e]	246	14.9	34.1	1.25
163	N	SC to OC	200 ± 4	11.7 ± 0.3	34.5 ± 0.3	0.80 ± 0.03
		OC to SC	198 ± 3	10.6 ± 0.5	34.2 ± 0.4	0.73 ± 0.06
		Best	204	11.8	34.6	0.83
	Y	SC to OC	237 ± 5	14.1 ± 0.4	35.1 ± 0.4	1.17 ± 0.05
		OC to SC	234 ± 6	13.8 ± 0.4	34.8 ± 0.5	1.13 ± 0.05
		Best	236	14.73	34.9	1.21

[a] Derived from the *J-V* curves (sweep rate 100 mV s^{-1}) for 10 devices of each type with an aperture of 0.16 cm^2 in all cases except for T_{dep} = 150 where apertures of 0.16 and 1.00 cm^2 were applied; V_{oc} – open circuit voltage, J_{sc} – short circuit current density, FF – fill factor, PCE – power conversion efficiency. [b] Solar cells without (N) and with (Y) MoO_3 evaporated on top of the spiro-OMeTAD layer. [c] Mean values and standard deviation derived from measurements from short-circuit (SC) to open-circuit (OC) and in the opposite direction (OC to SC). [d] Data for the best-performing solar cell measured in the SC to OC direction. [e] Data for the best-performing solar cell with a working area of 1 cm^2 measured in the SC to OC direction.

Table S4 (continued). Photovoltaic parameters[a] of the planar Ag|(MoO_3+)spiro-OMeTAD|$AgBiS_2$|ZnO|ITO solar cells with the light absorber obtained by spray pyrolysis at different temperatures under 1 sun AM1.5G irradiation.

T_{dep} (°C)	MoO_3 [b]		V_{oc} (mV)	J_{sc} (mA cm^{-2})	FF (%)	PCE (%)
175	N	SC to OC [c]	198 ± 5	9.9 ± 0.3	34.7 ± 0.3	0.68 ± 0.05
		OC to SC [c]	197 ± 2	9.6 ± 0.4	34.5 ± 0.4	0.66 ± 0.03
		Best [d]	201	10.7	35.1	0.76
	Y	SC to OC	234 ± 4	10.4 ± 0.3	35.6 ± 0.3	0.87 ± 0.03
		OC to SC	232 ± 3	10.3 ± 0.3	35.2 ± 0.3	0.84 ± 0.03
		Best	239	10.5	35.9	0.90
200	N	SC to OC	196 ± 4	7.8 ± 0.3	34.8 ± 0.3	0.53 ± 0.04
		OC to SC	193 ± 5	7.0 ± 0.5	34.7 ± 0.2	0.48 ± 0.05
		Best	200	8.2	35.4	0.58
	Y	SC to OC	231 ± 5	8.9 ± 0.4	36.0 ± 0.4	0.74 ± 0.07
		SC to OC [c]	198 ± 5	9.9 ± 0.3	34.7 ± 0.3	0.68 ± 0.05
		OC to SC [c]	197 ± 2	9.6 ± 0.4	34.5 ± 0.4	0.66 ± 0.03

[a] Derived from the *J-V* curves (sweep rate 100 mV s^{-1}) for 10 devices of each type with an aperture of 0.16 cm^2; V_{oc} – open circuit voltage, J_{sc} – short circuit current density, FF – fill factor, PCE – power conversion efficiency. [b] Solar cells without (N) and with (Y) MoO_3 evaporated on top of the spiro-OMeTAD layer. [c] Mean values and standard deviation derived from measurements from short-circuit (SC) to open-circuit (OC) and in the opposite direction (OC to SC). [d] Data for the best-performing solar cell measured in the SC to OC direction.

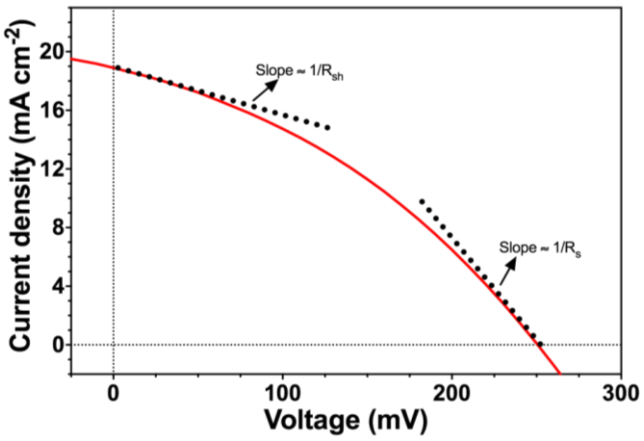

Figure S12. Estimation of the shunt (R_{sh}) and series (R_s) resistance by linear approximations (*black dotted lines*) to the *J-V* data (sweep rate 100 mV s^{-1}; 1 sun AM1.5G) for the Ag|MoO_3+spiro-OMeTAD|$AgBiS_2$|ZnO|ITO solar cell (aperture 0.16 cm^2) with the light-absorber layer spray-deposited at 150 °C.

Table S5. Series (R_S) and shunt (R_{sh}) resistance[a, b] for Ag|spiro-OMeTAD|$AgBiS_2$|ZnO|ITO solar cells with the light absorber layer obtained at different temperatures.

T_{dep} (°C)	MoO_3 [c]	R_{sh} [a] (Ω cm^{-2})	R_s [b] (Ω cm^{-2})
125	N	33	15
	Y	37	14
150	N	28	13
	Y	30	7.3
175	N	32	14
	Y	45	14

[a, b] Derived from the *J-V* data as exemplified in Figure S14. [c] Solar cells with (Y) and without (N) MoO_3 evaporated on top of the spiro-OMeTAD layer.

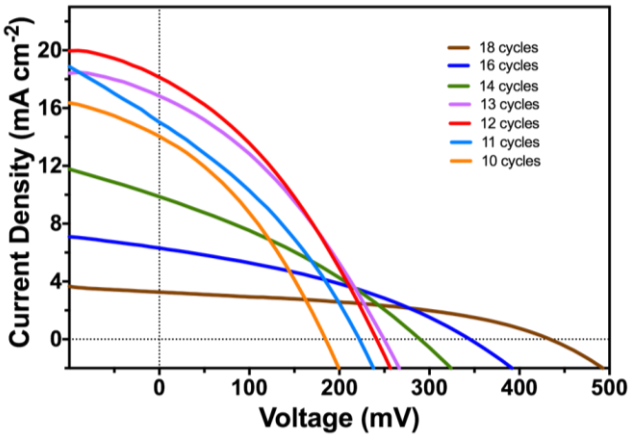

Figure S13. (a) Photocurrent-voltage curves (scan rate 100 mV s^{-1}; open-circuit to short-circuit sweeps are omitted for clarity) measured under 1 sun AM1.5G irradiation for the Ag|MoO_3+spiro-OMeTAD|$AgBiS_2$|ZnO|ITO devices (aperture 0.16 cm^2) with the light harvester layer spray-deposited at 150 °C for different number of deposition cycles.

Table S6. Photovoltaic performance[a] of the planar Ag|MoO_3+spiro-OMeTAD|$AgBiS_2$|ZnO|ITO solar cells with the light absorber layer obtained with different number of spraying cycles at T_{dep} =150 °C.

Number of deposition cycles[b]		V_{oc} (mV)	J_{SC} (mA cm^{-2})	FF (%)	PCE (%)
10	SC to OC[c]	187 ± 6	14.2 ± 0.2	32.2 ± 0.4	0.87 ± 0.05
	OC to SC[c]	184 ± 5	13.9 ± 0.4	31.8 ± 0.5	0.85 ± 0.06
11	SC to OC	222 ± 7	15.1 ± 0.6	33.0 ± 0.4	1.11 ± 0.08
	OC to SC	221 ± 4	14.6 ± 0.7	32.7 ± 0.5	1.08 ± 0.05
12	SC to OC	241 ± 7	18.1 ± 0.6	34.6 ± 0.5	1.50 ± 0.12
	OC to SC	239 ± 4	17.9 ± 0.5	34.4 ± 0.2	1.46 ± 0.07
13	SC to OC	253 ± 4	16.8 ± 0.4	34.1 ± 0.3	1.41 ± 0.05
	OC to SC	251 ± 5	16.7 ± 0.3	33.7 ± 0.4	1.39 ± 0.06
14	SC to OC	290 ± 3	9.9 ± 0.3	32.1 ± 0.5	0.92 ± 0.03
	OC to SC	287 ± 4	9.8 ± 0.4	31.9 ± 0.4	0.90 ± 0.04
16	SC to OC[c]	345 ± 5	6.3 ± 0.5	35.0 ± 0.3	0.75 ± 0.05
	OC to SC[d]	342 ± 5	5.9 ± 0.6	34.4 ± 0.5	0.70 ± 0.07
18	SC to OC[c]	434 ± 4	3.3 ± 0.7	42.1 ± 0.4	0.58 ± 0.06
	OC to SC[d]	431 ± 5	3.3 ± 0.5	41.9 ± 0.4	0.57 ± 0.05

[a] Derived from the *J-V* curves (sweep rate 100 mV s^{-1}) for 10 devices of each type with an aperture of 0.16 cm^2; V_{oc} - open circuit voltage, J_{sc} – short circuit current density, FF – fill factor, PCE – power conversion efficiency. [b] Solar cells fabricated by varying number of spraying cycles of $AgBiS_2$. [c] Mean values and standard deviations derived from measurements from short-circuit (SC) to open-circuit (OC) and in the opposite direction (OC to SC).

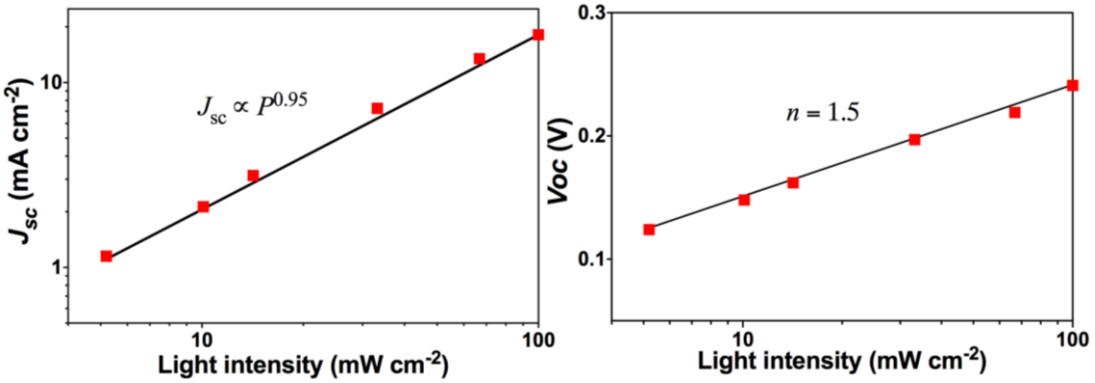

Figure S14. Dependence of (a) short-circuit current density and (b) open-circuit voltage for the Ag|MoO_3+spiro-OMeTAD|$AgBiS_2$|ZnO|ITO solar cells (T_{dep} = 150 °C; 12 spray cycles) on irradiation intensity (P). Solid lines show linear approximations to the experimental data. In panel **b**, the ideality factor n is calculated by the equation for free carrier transport proposed by Koster et al.[S3,S4]

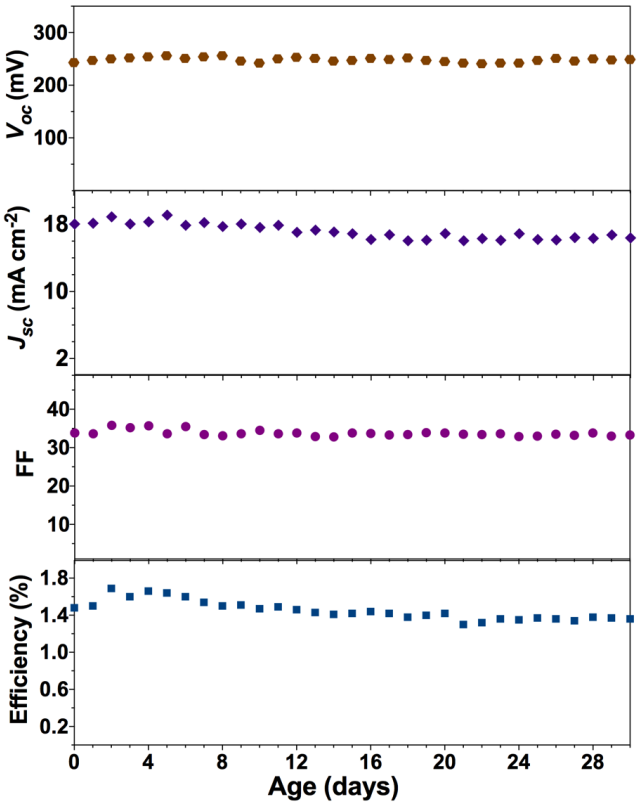

Figure S15. Evolution of the photovoltaic parameters of a non-encapsulated Au|MoO_3+spiro-OMeTAD|$AgBiS_2$|ZnO|ITO device stored on air under diffuse light for 1 month. The $AgBiS_2$ film was spray-deposited at 150 °C. Data were derived from *J-V* curves (scan rate 100 mV s^{-1}) recorded from short circuit to open circuit under 1 sun AM1.5G irradiation. Starting parameter values were V_{OC} =250 mV, J_{SC} = 17.6 mA cm^{-2}, FF = 33.8 %, PCE = 1.49 %.

SUPPLEMENTARY REFENRECES

S1. Shu, Y.; Mikosch, A.; Winzenberg, K. N.; Kemppinen, P.; Easton, C. D.; Bilic, A.; Forsyth, C. M.; Dunn, C. J.; Singh, T.; Collis, G. E., N -Alkyl functionalized barbituric and thiobarbituric acid bithiophene derivatives for vacuum deposited n-channel OFETs. *J. Mater. Chem. C* **2014,** *2*, 3895-3899.

S2. Bernechea, M.; Miller, N.; Xercavins, G.; So, D.; Stavrinadis, A.; Konstantatos, G., Solution-processed solar cells based on environmentally friendly $AgBiS_2$ nanocrystals. *Nat. Photon.* **2016,** *10*, 521-525.

S3. Koster, L. J. A.; Mihailetchi, V. D.; Ramaker, R.; Blom, P. W. M., Light intensity dependence of open-circuit voltage of polymer: fullerene solar cells. *Appl. Phys. Lett.* **2005,** *86*, 123509.

S4. Proctor, C. M.; Kuik, M.; Nguyen, T.-Q., Charge carrier recombination in organic solar cells. *Prog. Polym. Sci.* **2013,** *38*, 1941-1960.